Accepted Manuscript

Inducing stable interfacial delamination in a multilayer system by four-point bending of microbridges

James L. Mead, Mingyuan Lu, Han Huang

PII: S0257-8972(16)31201-4
DOI: doi: 10.1016/j.surfcoat.2016.11.069
Reference: SCT 21815

To appear in: *Surface & Coatings Technology*

Received date: 31 August 2016
Revised date: 16 November 2016
Accepted date: 18 November 2016

Please cite this article as: James L. Mead, Mingyuan Lu, Han Huang, Inducing stable interfacial delamination in a multilayer system by four-point bending of microbridges, *Surface & Coatings Technology* (2016), doi: 10.1016/j.surfcoat.2016.11.069

Inducing stable interfacial delamination in a multilayer system by four-point bending of microbridges

James L. Mead[a]

Email: james.mead@uqconnect.edu.au

Mingyuan Lu[a]

Email: mingyuan.lu@uqconnect.edu.au

Han Huang[a,*]

* Corresponding author: Tel.: +61 7 33653583; Fax: +61 7 33654799

Email: han.huang@uq.edu.au

Author postal address: School of Mechanical & Mining Engineering, Frank White Building (43), Level 2, The University of Queensland, QLD 4072 Australia

[a] School of Mechanical and Mining Engineering, The University of Queensland

Affiliation postal address: School of Mechanical & Mining Engineering, Frank White Building (43), Level 2, The University of Queensland, QLD 4072 Australia

Abstract

The ability to produce stable delamination of thin film multilayer interfaces is a powerful tool for studying the interfacial adhesion within microsystems. In this study, a technique involving the four-point bending of microbridges was applied to initiate stable interfacial delamination within a multilayer system. Microscale pre-notched bridges with clamped-ends were machined into an Al/SiN/GaAs multilayer using focus ion beam milling. A square flat-end indenter was used to induce bending of the bridge by two contact locations. Bridge failure occurred via substrate fracture at the pre-notch, followed by crack deflection, and stable interfacial delamination of the SiN/GaAs interface. Substrate fracture and delamination were identified within the obtained load-displacement curves as a pop-in and region of linear load reduction respectively.

Keywords: *thin film multilayer; interface; microbridge; four-point bending; nanoindentation; FIB milling*

1. Introduction

The interfacial adhesion of thin film multilayers is an important factor affecting the performance and service life of contemporary microelectronic devices as well as micro-electrical mechanical systems (MEMS). Delamination of the thin films can lead to significant reliability issues. For the design of robust microsystems, the ability to assess a particular interface within multilayers, particularly on the microscale, is crucial. Therefore, methods capable of isolating and inducing stable delamination events within multilayer interfaces are of considerable research importance.

One of the most widely accepted methods used for studying interfacial adhesion within thin film multilayers is four-point bending (4PB) [1, 2]. The method has been successfully used to evaluate a variety of 'blanket' multilayers [3-7]. However, in order to apply load to the specimen, the configuration is conventionally applied on the macroscale. Consequently, the method is often unable to isolate the microscale interfaces that exist within 'patterned' multilayers. Top surface [8-10], as well as cross-sectional nanoindentation [11-13] are methods that have proven effective at initiating microscale delamination in a variety of thin films and multilayers. However, the complex stress state induced in a specimen during an indent is accompanied by unavoidable plastic deformation [9]. As a result, the energy dissipated by plastic deformation is not easily decoupled from the total work. A 'test-specific' practical work of adhesion is therefore typically obtained [14].

Nanoindentation induced deformation of microscale structures fabricated using focused ion beam (FIB) milling has been increasingly utilised for investigating the properties of thin films [15, 16]. The deformation of a well-defined structure milled into a microscale feature of interest, allows the feature to be studied under a simple, quantifiable stress-state. For example, microcantilever (MC) bending has been used to investigate the elastic modulus [17], yield strength [18], fracture toughness [19, 20], fatigue properties [21], and residual stress [22, 23] of thin films. More recently, the fracture toughness of thin films and coatings have been assessed by means of micropillar splitting [24], double-cantilever compression [25], as well as three point bending of clamped bridges [26, 27].

A limited number of studies have applied the indentation of fabricated microscale structures to investigate interfaces [17, 28]. Matoy et al. [29], Hirakata et al. [30], and Chan et al. [31], used notched MC configurations to initiate delamination of SiO/W and SiO/Cu, Sn/Si, and Zr/hydride interfaces, respectively. Delamination generally occurred in an unstable manner due to the interfaces being orientated perpendicular to the axis of the MCs; prompting the development of alternative configurations [32].

This present work aimed to develop a microscale method capable of initiating stable interfacial delamination within a thin film multilayer by effectively miniaturising conventional 4PB. FIB milling was used to fabricate microbridges (MBs) within an Al/SiN/GaAs multilayer; a system considered typical of those found in microelectronic devices. A 4PB configuration was applied using a flat-end indenter in order to induce a linear-elastic stress state. This resulted in the initiation and deflection of a substrate crack, followed by stable delamination of the SiN/GaAs interface. The method is theoretically applicable to both blanket and patterned multilayers.

2. Methodology

2.1 Specimen preparation

An Al/SiN/GaAs multilayer specimen was synthesized for this study. Adhesion of the SiN/GaAs interface was of primary interest as delamination of the passivating SiN film has been a critical issue affecting the reliability of GaAs based microelectronics. Amorphous SiN film / single crystal (001) GaAs substrate specimens were provided by WIN Semiconductors Co. The SiN film was deposited by plasma enhanced chemical vapour deposition (PECVD); the details of which can be found elsewhere [8]. An aluminium film was deposited onto the SiN film by direct-current magnetron sputtering using an Auto 500 Sputter Coater (HHV Technologies. West Sussex, United Kingdom). Deposition was undertaken in an argon atmosphere at a base pressure of 4 mTorr, and a power range from 80 to 250 W.

2.2 Machining of microbridges

MBs were milled into the top surface of the specimens using a Scios DualBeam FIB (FEI, Oregon, USA). The detailed milling procedure can be found elsewhere [33, 34]. The MBs were examined using a 7100F scanning electron microscope (SEM) (JEOL Ltd., Tokyo, Japan). The fabricated MBs consisted of an Al layer, SiN layer, and GaAs substrate component with side wall heights of h_{Al}, $h_{SiN,}$ h_{GaAs} respectively. SEM micrographs of a typical MB are shown in Fig. 1(a); the resultant pentagonal cross-section is illustrated in Figure 1(b). MB dimensions, including length, L, and width, W, are summarised in Table 1. Wedge-shaped centered pre-notches of height, h_{notch}, with an included angle of 20°, were milled into the substrate component to promote fracture during bending. A milling current of

100pA resulted in an average notch root radius of 200 nm. Large fillets, with radii, R_{end}, ranging from 3-5 μm, were introduced on the clamped ends of each MB to avoid stress concentrations. A centrally located blind hole, further referred to as a 'centring hole', was milled into the top surface of each MB using a low milling current of 50 pA.

2.3 Nanoindentation

Nanoindentation induced bending of MBs was undertaken using a TI900 Triboindenter (Hysitron Inc., Minneapolis, USA). Bending was applied under a 4-point configuration using a 10 μm square flat-end indenter, whereby the opposite edges of the indenter acted as inner contact lines. A schematic of the experimental configuration is shown in Fig. 1(c). Alignment of the indenter was achieved by evaluating successive indentation impressions applied to an un-milled region of the sample surface. Tilt and rotational alignment of the indenter with each MB was evaluated using AFM and corrected using a tilt-stage. Positioning of the indenter on each MB was achieved by using the 'centring hole' as an optical reference. Indentation on all MBs were undertaken at a loading velocity 10 nm/s.

To allow for SEM examination of the MBs through each step of the fracture sequence, bending was applied incrementally over two separate indentations. During bending, once a particular feature was observed in the *P-h* data, the indenter was halted and withdrawn. The indenter withdrawal points were categorised into 3 distinct groups: withdrawals after a pop-in, [W1], withdrawals after a pop-in and subsequent decline in load, [W2], and withdrawals after a long term decline in load, [W3].

3. Results

The *P-h* curves for the 1st 4PB of MBs are shown in Fig. 2(a). At low displacements all MBs exhibited linear-elastic loading behaviour. At higher displacements all MBs gradually deviated from linearity, followed by the occurrence of a significant initial pop-in. Bending of MB1 and MB2 was then immediately halted. Loading of MB3 continued at a dramatically increased compliance. This was followed by a second significant pop-in, resulting in a load drop to approximately 1000 μN. Bending of MB3 was then immediately halted.

SEM examination was used to investigate the deformation behaviour of the MBs after the 1st indentation. MB1 and MB2 observations were indicative of the typical fracture state after the occurrence of an initial pop-in. MB3 observations were indicative of the typical fracture state after a second pop-in. Both fracture states are illustrated in Fig. 3(a) and (b). Substrate fracture was found to have initiated within the radius of the notch for all MBs. Propagation occurred at angles ranging from 0° to 45° from the vertical plane. For example, in MB1, a single substrate fracture was observed, terminating at the SiN / GaAs interface (Fig. 3(a)). In MB3, two substrate fractures were observed; one terminated at the interface, and the other deflected into the interface resulting in a short asymmetric interfacial delamination (Fig. 3(b)). An impression was observed on the Al surface of each MB due to the contact of the flat-end indenter. Analysis of these impressions indicated that a moderate indenter misalignment of 0.2 μm occurred during bending of each MB.

The *P-h* curves for the 2nd 4PB indentation of MBs are shown in Fig. 2(b). As per the 1st indentation, displacement of MB1 and MB2 initially demonstrated linear-elastic loading behaviour, followed by a gradual deviation from linearity. A significant pop-in occurred in both MBs, followed by a linear decline in load. Initial displacement of MB3 resulted in a linear increase in load similar to MB1 and MB2. At an approximate load of 1400 μN (exceeding the withdrawal load during the 1st indentation), the trend rapidly changed to a linear decline in load similar to that observed in MB1 and MB2. These regions were permitted to extend for between 300 to 800 nm prior to bending being halted.

SEM examination was used to investigate deformation behaviour of the MBs after the 2nd indentation. All MB observations were indicative of the typical fracture state after a region of declining load was observed. Comparison of the final state with the fracture state after an initial and second pop-in was undertaken by considering MB1 and MB3 independently. SEM micrographs of both MBs are shown in Fig. 3(c) and (d). In both MBs extensive asymmetrical delamination of the SiN/GaAs interface was observed. In MB1, delamination was achieved by the initiation and deflection of a second substrate fracture (Fig. 3(c) and (e)). In MB3, the delamination depicted in Fig 3(b) had continued to propagate in the same direction along the SiN/GaAs interface (Fig. 3(d)). New indentation impressions again indicated an indenter misalignment ranging from 0.4 and 1.5 μm respectively. A typical indentation impression is shown in Fig. 3(e).

4. Discussion

Correlation of the MB fracture states observed in the SEM micrographs (Fig. 3) with the respective *P-h* data (Fig. 2) allowed for a typical 'idealised' fracture sequence and corresponding *P-h* curve to be constructed. In literature, a fundamental analysis of the 4PB *P-*

h curves obtained from macroscale specimens is well-established [3, 35]. Nonetheless, it is important to investigate the *P-h* relationship unique to the clamped-end microscale specimens in this study. The typical MB fracture sequence, consisting of deformation / fracture steps from I to IV, is illustrated in Fig. 4.

During bending, load initially increased linearly with displacement as the MB deflected elastically (I). Once the elastic energy stored in the MB exceeded the fracture resistance of GaAs, a substrate crack initiated at the root of the notch and propagated towards the SiN/GaAs interface. The unstable fracture of the brittle substrate was reflected as a pop-in on the *P-h* curve (II). Deflection of a substrate fracture into the SiN/GaAs interface also required an accumulation of elastic energy. Once fracture deflection occurred, the release of strain energy allowed for short term unstable delamination of the interface until a dynamic equilibrium between the addition of strain energy and the resistance to delamination was reached [35]. The instability associated with fracture deflection and initial delamination was also represented by a pop-in (III).

After a dynamic equilibrium was reached the delamination continued in a stable manner. Ideally, if a highly symmetrical 4PB configuration was applied, a constant moment would be induced in the MB between the inner loading lines. Consequently, the stress-state at the crack tip during delamination would be independent of the delamination length. Delamination would therefore produce a region of constant load, or plateau, on the *P-h* curve. If a misaligned 4PB configuration was applied and / or delamination occurred asymmetrically, the stress-state at the crack tip during delamination would not remain constant. Delamination would therefore be reflected as a gradual increase or decrease in load (IV).

Uncertainty exists regarding whether substrate fracture and deflection into the interface always occurred as a single, or as separate unstable events. If the release of accumulated strain energy during substrate fracture was able to exceed the resistance to the deflection, then both (II) and (III) would be represented as a single pop-in. Otherwise, further accumulation of strain energy would be required for deflection, characterised by a region of increasing load prior to an additional pop-in. The initiation of additional substrate fractures was regularly preferred over the deflection of an existing substrate fracture, and therefore generated supplementary pop-ins. As a result, the *P-h* curve obtained for a given MB was able to exhibit multiple initial pop-ins associated with substrate fractures prior to a final pop-in associated with fracture deflection.

The *P-h* curves for the 1st and 2nd MB indentations agreed well with the 'idealised' model in Fig. 4, with the exception of two characteristics: (1) non-linear loading behaviour at high loads, and (2) a steady reduction in load during delamination. The deviation from linearity during loading was attributed to deformation at the clamped-ends of each MB. At each end, the applied 4PB configuration induced high tensile bending stresses at the top Al surface. The shallow indentation impressions observed on the top surface of each MB demonstrated that the amount of plastic deformation associated with indenter contact was negligible. Extensive elastic recovery during indenter withdrawal demonstrated that the primary contribution to indenter displacement was linear-elastic MB deflection.

The asymmetrical delamination events observed in the MBs always proceeded in the direction requiring the smallest angle of deflection for a given substrate fracture. A recent MB bending study of a PtNiAl bond coat system revealed that indenter misalignment resulted in fracture propagation in the direction of maximum tangential stress [36]. Conversely, in this study, both substrate fracture and delamination typically did not proceed in the direction of increasing

moment gradient. This indicated that asymmetrical delamination may have been dependent on the initiating substrate fracture, which in turn would have be influenced by the crystallographic orientation of the single crystal GaAs substrate. As indenter misalignment was limited to under 1.5 μm in this work, a near symmetric 4PB stress-state was assumed when the length of delamination was small.

The proposed MB 4PB technique has proven to be effective at inducing microscale interfacial delamination within a multilayer. The technique provides some distinctive advantages over similar microscale methods. Of particular significance is the bending moment distribution induced along the MB under 4PB, which allows for the investigation of stable delamination. Furthermore, the well-defined MB geometry permits simplified modelling of the deformation response. In future studies, the strain energy stored within the MB at a given indenter load can be determined analytically by considering the resultant MB deflection. The strain energy released during the delamination of an interface can then be derived by evaluating the strain energy stored within a unit cross-section of a MB before and after delamination [1]. Other than being small, the interfaces found within microelectronics and MEMS are often embedded deep within a multilayer structure, and therefore may not be conventionally accessible. Adjusting the milled height of a MB as well as the stop position of the notch dictates which layers are subjected to deformation and which interface is first exposed to the initiated intralayer fracture. The MB machining process therefore offers the ability to isolate and potentially delaminate specific embedded interfaces. However, in regards to the technique's applicability to other multilayer systems, two potential limitations must be considered. First, in systems containing brittle layers, buckling or fracture of the layer may occur in locations of high tensile stress away from the notch. Second, the tendency for an intralayer fracture to deflect into or penetrate the interface of interest is governed by the following; 1) the relative stiffness of adjacent layers, 2) the toughness ratio between the interface and the opposite

adjacent layer, and 3) the angle of the approaching intralayer fracture [37]. Consequently, in systems where the interface of interest is tough, the initiated intralayer fracture may always preferentially penetrate the interface so that delamination cannot be achieved.

5. Conclusions

The four-point bending of microbridges was developed as a viable technique for initiating interfacial delamination within thin film multilayers. The configuration proposed involved the loading of FIB milled clamped-end microbridges using a square flat-ended indenter. SEM observations showed that delamination of the SiN/GaAs interface was successfully initiated via substrate fracture at the notch, followed by fracture deflection. Analysis of the obtained load-displacement curves identified substrate fracture and interfacial delamination as pop-ins and a region of linear load reduction respectively. The load of delamination decreased with increasing delamination length. This was attributed to a moment gradient introduced by indenter misalignment and asymmetrical delamination. Nevertheless, a near symmetric four-point bending stress-state was assumed for small delamination lengths. A significant advantage that the four-point bending configuration provides in comparison to similar microscale methods is the capability to investigate stable delamination events. This allows for an improved understanding of adhesion within the embedded interfaces of both blanket and patterned multilayers.

Acknowledgements

This author would like to acknowledge the facilities, and the scientific and technical assistance, of the Australian Microscopy and Microanalysis Research Facility at the Centre for Microscopy and Microanalysis, The University of Queensland.

HH is supported by the Australian Research Council (ARC) under the Future Fellowship program (FT110100557).

References

[1] P.G. Charalambides, J. Lund, A.G. Evans, R.M. McMeeking, A Test Specimen for Determining the Fracture Resistance of Bimaterial Interfaces, Journal of Applied Mechanics, 56 (1989) 77-82.

[2] P.G. Charalambides, H.C. Cao, J. Lund, A.G. Evans, Development of a test method for measuring the mixed mode fracture resistance of bimaterial interfaces, Mechanics of Materials, 8 (1990) 269-283.

[3] Q. Ma, A four-point bending technique for studying subcritical crack growth in thin films and at interfaces, Journal of Materials Research, 12 (1997) 840-845.

[4] R.H. Dauskardt, M. Lane, Q. Ma, N. Krishna, Adhesion and debonding of multi-layer thin film structures, Engineering Fracture Mechanics, 61 (1998) 141-162.

[5] P.F. Zhao, C.A. Sun, X.Y. Zhu, F.L. Shang, C.J. Li, Fracture toughness measurements of plasma-sprayed thermal barrier coatings using a modified four-point bending method, Surface and Coatings Technology, 204 (2010) 4066-4074.

[6] B. Völker, S. Venkatesan, W. Heinz, K. Matoy, R. Roth, J.-M. Batke, M.J. Cordill, G. Dehm, Following crack path selection in multifilm structures with weak and strong interfaces by in situ 4-point-bending, Journal of Materials Research, 30 (2015) 1090-1097.

[7] S. Brinckmann, B. Völker, G. Dehm, Crack deflection in multi-layered four-point bending samples, Int J Fract, 190 (2014) 167-176.

[8] M. Lu, H. Huang, Interfacial energy release rates of SiN/GaAs film/substrate systems determined using a cyclic loading dual-indentation method, Thin Solid Films, 589 (2015) 822-830.

[9] M. Lu, H. Huang, Determination of the energy release rate in the interfacial delamination of silicon nitride film on gallium arsenide substrate via nanoindentation, Journal of Materials Research, 29 (2014) 801-810.

[10] M.P. De Boer, W.W. Gerberich, Microwedge indentation of the thin film fine line—II. Experiment, Acta Materialia, 44 (1996) 3177-3187.

[11] I. Ocaña, J.M. Molina-Aldareguia, D. Gonzalez, M.R. Elizalde, J.M. Sánchez, J.M. Martínez-Esnaola, J. Gil Sevillano, T. Scherban, D. Pantuso, B. Sun, G. Xu, B. Miner, J. He, J. Maiz, Fracture characterization in patterned thin films by cross-sectional nanoindentation, Acta Materialia, 54 (2006) 3453-3462.

[12] J.M. Sánchez, S. El-Mansy, B. Sun, T. Scherban, N. Fang, D. Pantuso, W. Ford, M.R. Elizalde, J.M. Martínez-Esnaola, A. Martín-Meizoso, J. Gil-Sevillano, M. Fuentes, J. Maiz, Cross-sectional nanoindentation: a new technique for thin film interfacial adhesion characterization, Acta Materialia, 47 (1999) 4405-4413.

[13] X. Wang, C. Wang, A. Atkinson, Interface fracture toughness in thermal barrier coatings by cross-sectional indentation, Acta Materialia, 60 (2012) 6152-6163.

[14] A.A. Volinsky, N.R. Moody, W.W. Gerberich, Interfacial toughness measurements for thin films on substrates, Acta Materialia, 50 (2002) 441-466.

[15] K. Matoy, H. Schönherr, T. Detzel, T. Schöberl, R. Pippan, C. Motz, G. Dehm, A comparative micro-cantilever study of the mechanical behavior of silicon based passivation films, Thin Solid Films, 518 (2009) 247-256.

[16] D. Jang, L.R. Meza, F. Greer, J.R. Greer, Fabrication and deformation of three-dimensional hollow ceramic nanostructures, Nat Mater, 12 (2013) 893-898.

[17] S.F. Hwang, J.H. Yu, B.J. Lai, H.K. Liu, Young's modulus and interlaminar fracture toughness of SU-8 film on silicon wafer, Mechanics of Materials, 40 (2008) 658-664.

[18] T.P. Weihs, S. Hong, J.C. Bravman, W.D. Nix, Mechanical deflection of cantilever microbeams: A new technique for testing the mechanical properties of thin films, Journal of Materials Research, 3 (1988) 931-942.

[19] S. Massl, W. Thomma, J. Keckes, R. Pippan, Investigation of fracture properties of magnetron-sputtered TiN films by means of a FIB-based cantilever bending technique, Acta Materialia, 57 (2009) 1768-1776.

[20] S. Johansson, F. Ericson, J.Å. Schweitz, Influence of surface coatings on elasticity, residual stresses, and fracture properties of silicon microelements, Journal of Applied Physics, 65 (1989) 122-128.

[21] K. Takashima, Y. Higo, Fatigue and fracture of a Ni–P amorphous alloy thin film on the micrometer scale, Fatigue & Fracture of Engineering Materials & Structures, 28 (2005) 703-710.

[22] S. Massl, J. Keckes, R. Pippan, A direct method of determining complex depth profiles of residual stresses in thin films on a nanoscale, Acta Materialia, 55 (2007) 4835-4844.

[23] R. Schöngrundner, R. Treml, T. Antretter, D. Kozic, W. Ecker, D. Kiener, R. Brunner, Critical assessment of the determination of residual stress profiles in thin films by means of the ion beam layer removal method, Thin Solid Films, 564 (2014) 321-330.

[24] M. Sebastiani, K.E. Johanns, E.G. Herbert, F. Carassiti, G.M. Pharr, A novel pillar indentation splitting test for measuring fracture toughness of thin ceramic coatings, Philosophical Magazine, 95 (2015) 1928-1944.

[25] S. Liu, J.M. Wheeler, P.R. Howie, X.T. Zeng, J. Michler, W.J. Clegg, Measuring the fracture resistance of hard coatings, Applied Physics Letters, 102 (2013) 171907.

[26] N. Jaya B, V. Jayaram, S.K. Biswas, A new method for fracture toughness determination of graded (Pt,Ni)Al bond coats by microbeam bend tests, Philosophical Magazine, 92 (2012) 3326-3345.

[27] Y. Hu, J.-H. Huang, J.-M. Zuo, In situ characterization of fracture toughness and dynamics of nanocrystalline titanium nitride films, Journal of Materials Research, 31 (2016) 370-379.

[28] M. Lu, J. Mead, Y. Wu, H. Russell, H. Huang, A study of the deformation and failure mechanisms of protective intermetallic coatings on AZ91 Mg alloys using microcantilever bending, Materials Characterization, 120 (2016) 337-344.

[29] K. Matoy, T. Detzel, M. Müller, C. Motz, G. Dehm, Interface fracture properties of thin films studied by using the micro-cantilever deflection technique, Surface and Coatings Technology, 204 (2009) 878-881.

[30] H. Hirakata, T. Hirako, Y. Takahashi, Y. Matsuoka, T. Kitamura, Creep crack initiation at a free edge of an interface between submicron thick elements, Engineering Fracture Mechanics, 75 (2008) 2907-2920.

[31] H. Chan, S.G. Roberts, J. Gong, Micro-scale fracture experiments on zirconium hydrides and phase boundaries, Journal of Nuclear Materials, 475 (2016) 105-112.

[32] B.N. Jaya, C. Kirchlechner, G. Dehm, Can microscale fracture tests provide reliable fracture toughness values? A case study in silicon, Journal of Materials Research, 30 (2015) 686-698.

[33] M. Lu, H. Russell, H. Huang, Fracture strength characterization of protective intermetallic coatings on AZ91E Mg alloys using FIB-machined microcantilever bending technique, Journal of Materials Research, 30 (2015) 1678-1685.

[34] D. Di Maio, S.G. Roberts, Measuring fracture toughness of coatings using focused-ion-beam-machined microbeams, Journal of Materials Research, 20 (2005) 299-302.

[35] R. Shaviv, S. Roham, P. Woytowitz, Optimizing the precision of the four-point bend test for the measurement of thin film adhesion, Microelectronic Engineering, 82 (2005) 99-112.

[36] B.N. Jaya, S. Bhowmick, S.A.S. Asif, O.L. Warren, V. Jayaram, Optimization of clamped beam geometry for fracture toughness testing of micron-scale samples, Philosophical Magazine, 95 (2015) 1945-1966.

[37] H. Ming-Yuan, J.W. Hutchinson, Crack deflection at an interface between dissimilar elastic materials, International Journal of Solids and Structures, 25 (1989) 1053-1067.

Table I

Dimensions of fabricated microbridges.

	MB1	MB2	MB3
$L\ (\mu m)$	34.53	34.08	26.56
$W\ (\mu m)$	3.606	3.438	2.919
$h_{GaAs}\ (\mu m)$	1.825	2.048	1.334
$h_{SiN}\ (\mu m)$	0.443	0.443	0.443
$h_{Al}\ (\mu m)$	0.751	0.751	0.675
$h_{notch}\ (\mu m)$	1.276	1.463	0.942
$R_{end}\ (\mu m)$	3.338	3.55	4.639

Fig. 1. (a) SEM micrographs of a typical FIB-milled MB (MB1) viewed at 45° tilt. Al, SiN, and GaAs components are labelled. (b) Indicative MB cross-section. (c) Schematic illustration of the 4PB experimental configuration.

Fig. 2. (a) P-h curves for the 1st 4PB indentation of MBs. Bending of MB1 and MB2 was halted after a single pop-in was observed [W1]. Bending of MB3 was halted after a second pop-in was observed [W2]. (b) P-h curves for the 2nd indentation of MBs. Bending of all MBs was halted after a region of linear load reduction was observed [W3]. An asterix symbol followed by a dashed-line signifies a pop-in. Features are labelled according to the established fracture sequence: (I) linear-elasticity, (II) initiation of a substrate fracture, (III) fracture deflection, and (IV) stable delamination of the SiN/GaAs interface. Fitting lines were produced by applying a Butterworth filter to segmented data.

Fig. 3. SEM micrographs of (a) MB1 and (b) MB3 after the 1st 4PB indentation. MB1 shows the typical fracture state after a single pop-in was observed [W1]. MB3 shows the typical fracture state after a second pop-in was observed [W2]. SEM micrographs of (c, e) MB1 and (d) MB3 after the 2nd 4PB indentation. Both MB1 and MB3 show the typical fracture state after a region of declining load was observed [W3]. (e) Typical indentation impressions on the Al surface of a MB (MB1 post-2nd indent).

Fig 4. Indicative P-h curve and fracture sequence during 4PB of MBs. Deformation / fracture events include, (I) linear-elasticity, (II) initiation of a substrate fracture, (III) fracture deflection, and (IV) stable delamination of the SiN/GaAs interface. Indenter withdrawal points, [W1], [W2], and [W3], are indicated. Broken lines refer to the loading / unloading curve for when the indenter is withdrawn after an initial and final pop-in.

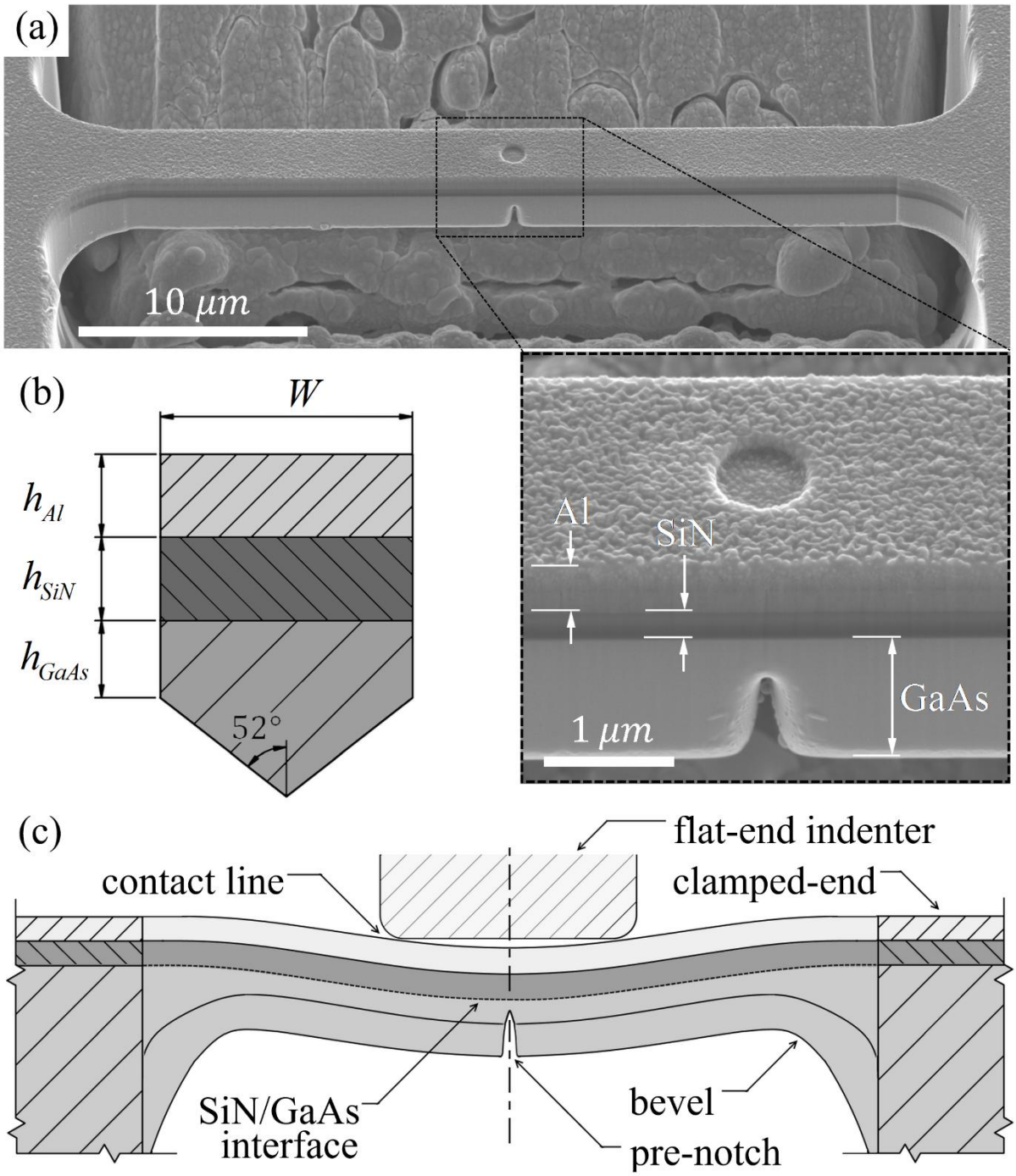

Figure. 1

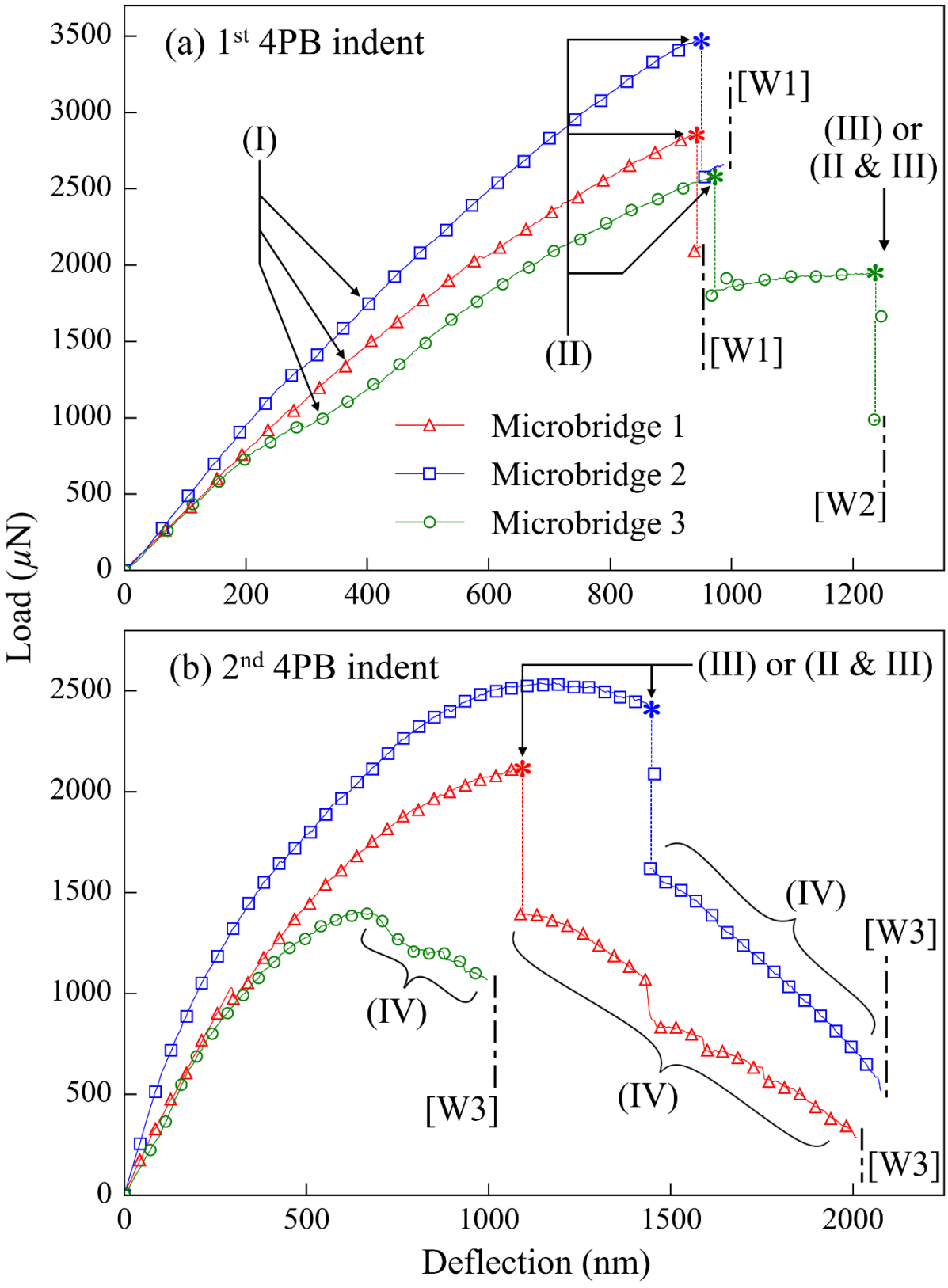

Figure. 2

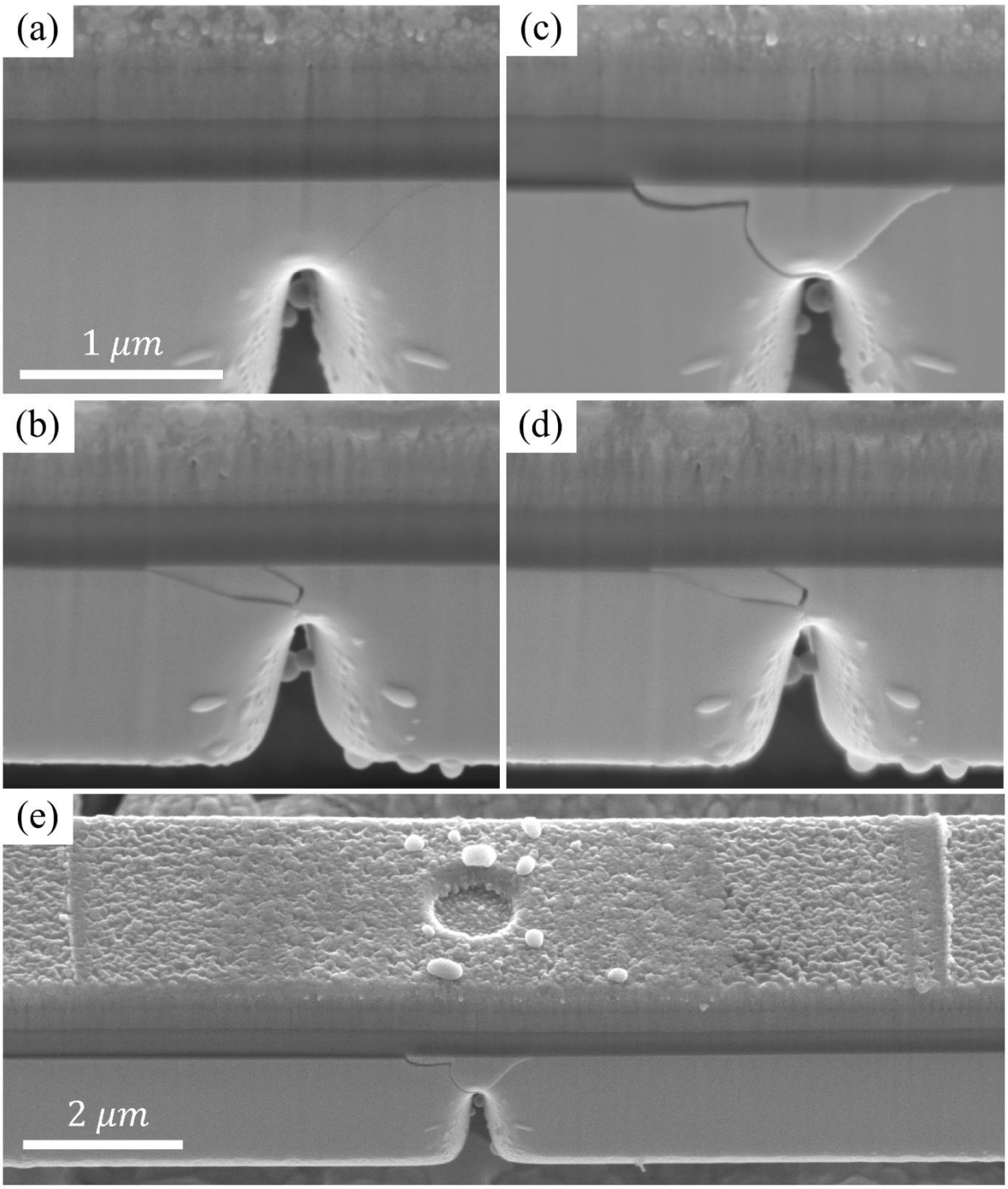

Figure. 3

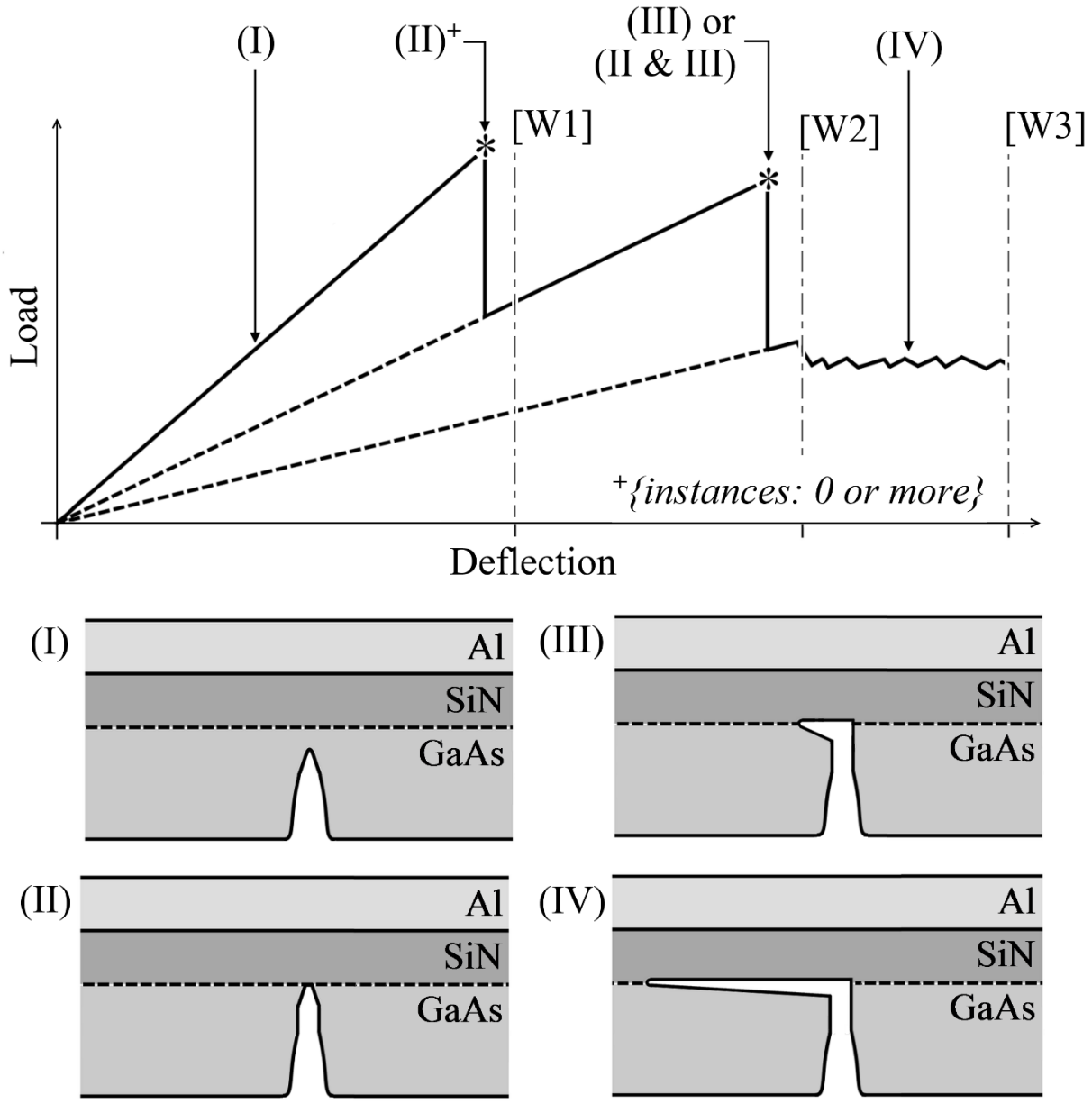

Figure. 4

Highlights (for review)

- A microbridge bending technique is proposed for studying the multilayer interfaces.
- Method is effective at induce ‘stable’ delamination in microscale interfaces.
- Mechanism involves fracture at pre-notch, and deflection into SiN/GaAs interface.
- Delamination corresponded to a region of load decline on load-displacement curve.
- Simple stress-state in precise geometry gives potential for quantitative analysis.